Available online at www.sciencedirect.com
ScienceDirect
Journal of Power Sources 158 (2006) 1270–1281
JOURNAL OF POWER SOURCES
www.elsevier.com/locate/jpowsour

Sulfonated polystyrene-type plasma-polymerized membranes for miniature direct methanol fuel cells

Stéphanie Roualdes *, Ionut Topala, Habiba Mahdjoub, Vincent Rouessac, Philippe Sistat, Jean Durand

Institut Européen des Membranes (UMR 5635), Université Montpellier II, CC 047 Place Eugene Bataillon, 34095 Montpellier Cedex 5, France

Received 11 May 2005; received in revised form 30 August 2005; accepted 13 October 2005
Available online 7 December 2005

Abstract

Sulfonated polystyrene-type membranes were synthesized by plasma polymerization of a mixture of styrene and trifluoromethane sulfonic acid monomers in a low-frequency after-glow discharge plasma reactor. Such a deposition process enables the preservation of the monomers structure, which was confirmed by mass spectrometry analysis. The synthesized plasma-polymerized membranes are dense and uniform with a few microns thickness. Their structure determined by Fourier-transform infra-red spectroscopy and X-ray photoelectron spectroscopy is very rich in sulfonic acid groups (up to 5%) and stable up to 120 °C. Even if their intrinsic proton conductivity is low (10^{-1} mS cm^{-1}), directly related to their disorganized and highly cross-linked structure, plasma-polymerized membranes present a proton conduction ability similar to Nafion® because of their low thickness. Due to their highly cross-linked structure, these membranes enable a reduction of the methanol crossover in a factor 10 by comparison with Nafion®. Thus, the integration of plasma-polymerized films in miniaturized direct methanol fuel cells as proton-exchange membranes seems promising.

Keywords: Plasma polymerization; Mass spectrometry; Fourier-transformed infra-red spectroscopy; Quartz crystal microbalance; Direct methanol fuel cell; Methanol crossover

1. Introduction

Recently, significant interest has been shown in the development of miniature fuel cells for portable devices. Among the different fuel cells, the polymer electrolyte membrane fuel cell offers the advantage of a compact device working at low temperatures. Hydrogen and methanol are the common fuels. The use of methanol is attractive for portable power sources because of its simple liquid fuel handling, improved safety and high energy density by comparison with hydrogen. The direct methanol fuel cell (DMFC) usually operates with the commercially available perfluorosulfonate ionomers membrane, such as Nafion®, formed of fluorocarboned chains with perfluorinated side chains containing sulfonic acid groups. Although Nafion® membranes are known as good proton-exchange membranes with quite high chemical and thermal stabilities, some weaknesses have been reported, such as material cost, relatively high membrane thickness, difficult humidity control, weak mechanical property and high methanol crossover. The crossover of methanol through the membrane which causes the reduction of fuel utilization efficiencies and cathode performance is a particularly limiting disadvantage. A number of approaches have been reported for reducing the crossover of methanol, ranging from the modification of existing membranes, firstly the Nafion® (surface treatments [1–9], manufacture of composite membranes [10,11]), to the development of new kind of membranes [12–18]. Among all these new membranes, Nafion® coated with a polybenzimidazole film has shown the best performance with a crossover reduced in a factor 2 [18]. Even if the reduction of crossover has been achieved, the competitiveness of such new membranes has not been yet demonstrated in DMFC for one of the following reasons: their conductivity is two low, the contact with the electrodes is not properly assured, and their life time is not sufficient [14,19–21]. Therefore, the use of membranes different from Nafion® remains yet limited in DMFCs. For microfuel cell applications, many studies have been recently

* Corresponding author. Tel.: +33 4 67 14 91 81; fax: +33 4 67 14 91 19.
E-mail address: Stephanie.Roualdes@iemm.univ-montp2.fr (S. Roualdes).

0378-7753/$ – see front matter © 2005 Elsevier B.V. All rights reserved.
doi:10.1016/j.jpowsour.2005.10.047

performed on the preparation of ionically conductive thin films by plasma polymerization. Materials prepared by plasma polymerization are thin, dense and amorphous three-dimensional matrices whose microstructural characteristics (morphology, chemical composition) can be modulated by modifying the main process parameters. Plasma polymers are very attractive membranes for microfuel cells due to many advantages inherent to the plasma synthesis technique. The two main advantages are: a micrometric thickness allowing an easy miniaturization and a strong adhesion on electrodes and a very highly cross-linked structure which gives them on one hand a very good chemical and thermal stability and on the other hand a very low permeability to organic liquids. Plasma polymers reported in the literature contain sulfonic, carboxylic or phosphoric acid groups as proton-exchange functions with a high proton permselectivity [22,23]. In general, the intrinsic ionic conductivities of plasma-polymerized membranes (4.3×10^{-2}–$0.58\,mS\,cm^{-1}$) are lower than that of Nafion® membranes (10–$100\,mS\,cm^{-1}$) but their conduction ability is observed to be competitive due to their low thickness [24,25]. Due to their highly cross-linked structure, plasma-polymerized membranes show methanol permeability much lower than that of Nafion® membranes [26–28].

In this work, polystyrene-type plasma polymers containing sulfonic acid groups were prepared by plasma polymerization from a gaseous mixture composed of styrene and trifluoromethane sulfonic acid (CF_3SO_3H) monomers. The role of the styrene monomer is to constitute the skeleton element of the carbonated polymer matrix; the role of the CF_3SO_3H monomer is to bring the proton conductive functions $–SO_3^-$. A previous study from our group has shown that a post-discharge configuration enables to obtain plasma polymers exhibiting higher sulfonic acid group contents and lower densities (directly related to higher phenyl-based group contents) by comparison with plasma materials synthesized in a direct glow discharge configuration [29]. Consequently, plasma polymers in this study were deposited in an after glow discharge system ensuring a good preservation of the monomers structure in polymer materials. The nature of fragments of monomers in the plasma phase, whose recombination leads to the formation of plasma polymers, was investigated using mass spectrometry (MS). Morphology and thickness of plasma-polymerized membranes were characterized using scanning electron microscopy (SEM). Chemical structure of plasma materials was determined using X-ray photoelectron spectroscopy (XPS) and Fourier-transform infra-red spectroscopy (FTIR). FTIR was also used to investigate the thermal stability of plasma materials. Density of materials was measured using small angle X-ray reflectometry. The proton conductivity of plasma-polymerized membranes was investigated by electrochemical impedance spectroscopy and proton transport number measurement. Measurements of methanol sorption and methanol diffusion permeability were performed using a quartz crystal microbalance and a Hittorf diffusion cell coupled to infrared spectroscopy, respectively.

The aim of this work is to establish correlations between the composition of the plasma phase, the microstructural characteristics of the synthesized plasma polymers (morphology, density, chemical structure) and their transport properties (proton conductivity and methanol permeability) in order to evaluate their potential as an alternative to Nafion® in DMFCs.

2. Experimental

2.1. Preparation of plasma-polymerized membranes

Plasma polymers were prepared in a low-frequency capacitively coupled reactor in stainless steel connected to a vacuum system (primary pump Leybold Trivac D40B). The reactor, depicted in Fig. 1, was in a post-discharge configuration; indeed the glow discharge was produced in the upper part of the reactor (Pyrex glass tube) whereas the film deposition was performed in the lower part of it (deposition chamber) where precursors were introduced. A butterfly valve driven by a pressure gauge (Tylan MDC) was placed between the deposition chamber and the vacuum pump in order to control the total pressure in the reactor. A liquid nitrogen trap was placed upstream from the vacuum pump to avoid contamination of the pump oil by unreacted monomers. The plasma discharge was sustained by a 40 kHz power supply (Alsatherm) between two external electrodes (5 cm gap) in a Pyrex glass tube (upper part of the reactor), using Ar (supplied by Air Liquide) as working gas. Gas lines allowed introducing the monomers in the deposition region (lower part of the reactor). Trifluoromethane sulfonic acid (CF_3SO_3H) and styrene, supplied by Aldrich, were used as monomers without any further purification. The monomers flow rates were controlled by a gas-handling system (H_2 as carrier gas) due to their high condensability. In order to avoid the polymerization and/or condensation of monomers on the inner walls of the gas lines, heating wires were wrapped around them. The substrate-holder in the deposition region was polarized in order to make easier the extraction of Ar^+ ions from the plasma region to the deposition region. The process parameters which were varied were: the input power supplied by the generator, the total pressure in the deposition chamber, the polarization value of the substrate-holder and the monomers flow rates (controlled by the partial pressure values). In a first step, deposition tests enabled to display optimum values for the first three parameters: 50 W for the input power, 0.5 mbar for the reactor total pressure and −10 V for the substrate-holder polarization. In a second step, these values were fixed and three different kind of membranes were synthesized from the following monomers mixtures: styrene (0.04 mbar)/CF_3SO_3H (0.04 mbar), styrene (0.04 mbar)/CF_3SO_3H (0.14 mbar), styrene (0.04 mbar)/CF_3SO_3H(0.18 mbar). In the following parts plasma films will be named using the acronym StCFa with St and CF indicating styrene and trifluoromethane sulfonic acid monomers and a being the ratio of the partial pressure of CF_3SO_3H to the partial pressure of styrene (a is equal to 1, 3.5 or 4.5 for the first, second or third mixture, respectively).

The different substrates used to support plasma-polymerized films were: standard gas diffusion layers (E-TEK) or silicon wafers (p-doped Si(1 0 0)) for SEM observations, silicon wafers for microstructural characterizations, silicon wafers covered with a thin film of gold for conductivity measurements, PVDF porous substrates for methanol diffusion measurements and quartz supports for methanol sorption measurements. It has been

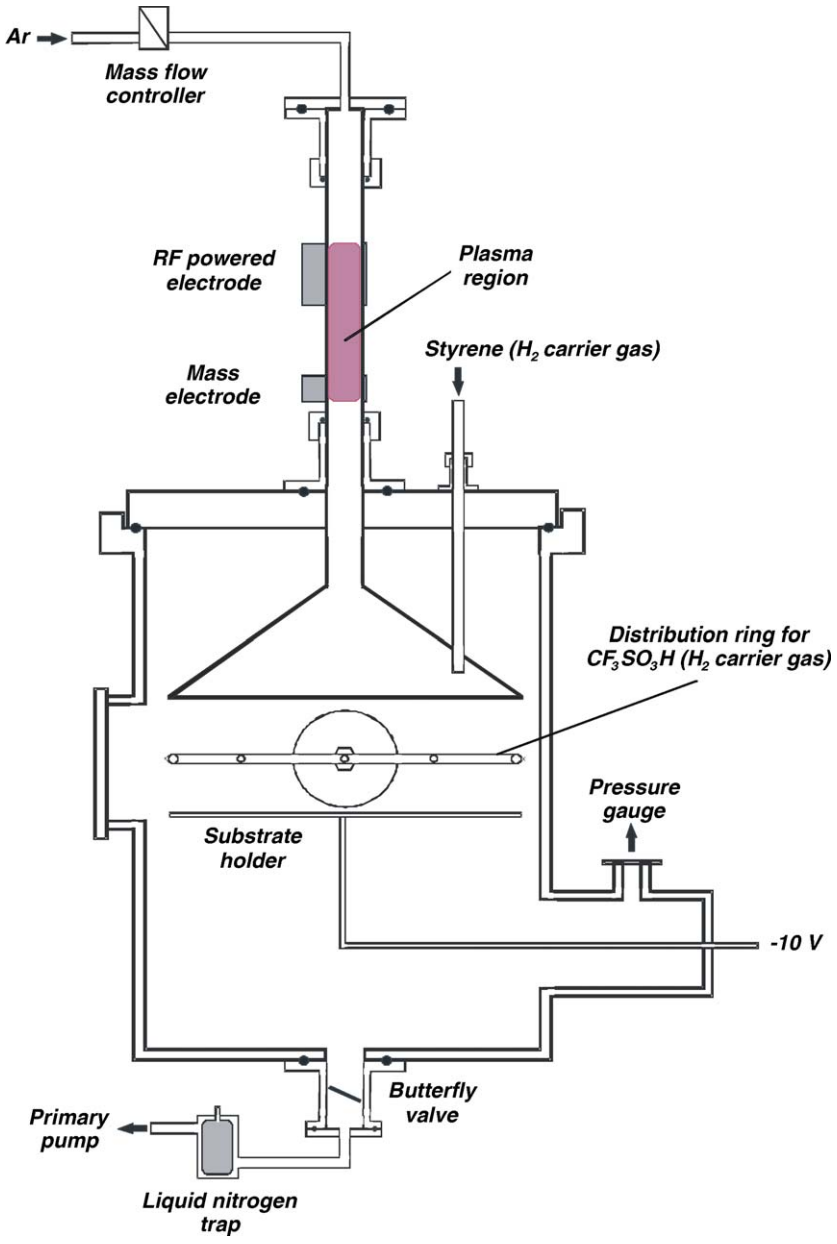

Fig. 1. Schematic diagram of the plasma polymerization reactor.

previously shown that the support nature does not affect the chemical structure of plasma-polymerized films [29].

2.2. Mass spectrometry for the characterization of the plasma phase

MS was used in order to understand the fragmentation process of monomers in the plasma-polymerization reactor. In situ MS experiments were performed using a Hiden EQP300 (range 1–300 amu, ionization energy 1–70 eV) apparatus attached to a specific plasma reactor (Fig. 2). The plasma discharge was sustained between two stainless steel circular electrodes (10.5 cm diameter, 2 cm gap) by a 40 kHz power supply (Alsatherm) using Ar as working gas, with 55 μbar partial pressure. The styrene and CF_3SO_3H monomers were separately introduced in the electrode gap using H_2 as carrier gas. The mass spectrometer's probe, pointing the electrodes gaps, can extract species through a 50 μm orifice by a differential pumping to maintain the pressure in the mass spectrometer below 10^{-6} mbar. In order to keep a low pressure in the mass spectrometer, the maximal total pressure in the reactor was regulated at 200 μbar by a butterfly valve, driven by a pressure gauge (Tylan MDC), independently on the gases flow rates. The mass spectrometer was used under residual gas analysis (RGA) mode which means that neutral species (molecules and radicals) of the plasma phase were extracted by differential pumping and then ionized (ionization energy: 25 eV) to be detected. The power supply was first operating with a 100 Hz modulation (every 10 ms, a 40 kHz signal was applied for 1.2 ms, no signal was applied for 8.8 ms) in order to obtain a low dissipated power in the range 1.5–7 W. Such power values correspond

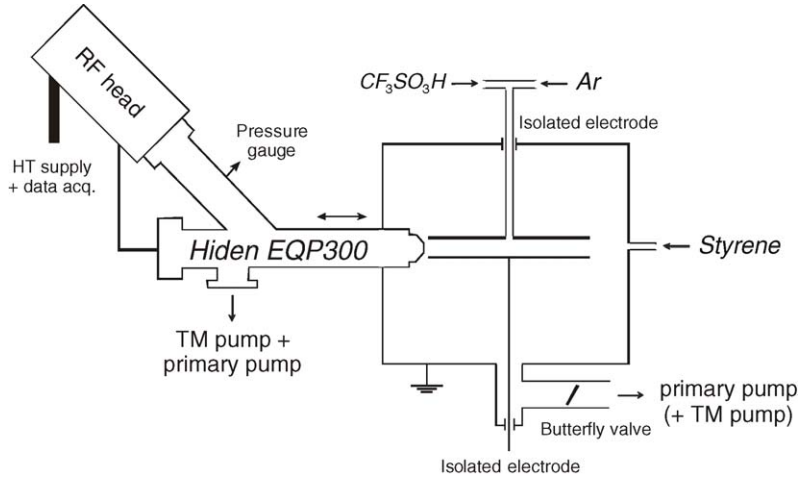

Fig. 2. Experimental set-up for mass spectrometry analysis; HT, high tension; TM, turbomolecular.

to soft plasma conditions, such as that supplied in reactors with a post-discharge configuration. The operation without any modulation, enabling to obtain a high dissipated power equal to 40 W (such as that supplied in direct glow discharges), was also tested as a comparison.

2.3. Microstructural characterizations of plasma polymers

Thickness and morphology of plasma polymers were determined from pictures of materials using a scanning electron microscope S-4500 Hitachi. The films density was evaluated by small-angle X-ray reflectometry measurements using a Siemens D5000 apparatus. FTIR, using a Nicolet Impact 400D spectrometer, in the range 4000–400 cm^{-1} (64 scans with 2 cm^{-1} resolution) and XPS, using a Cameca Ribber UHV device working with a MAC2 electron spectrometer, were used to investigate the films chemical structure. FTIR analysis coupled wilh a temperature cell (Graseby Specac) connected to a primary vacuum pump was used to determine the thermal stability of plasma materials up to 120 °C. For this study, the domain 520–400 cm^{-1} was eliminated because of strong absorbance of temperature cell windows; the resolution was 1 cm^{-1}. Each analyzed sample was thermally equilibrated for 30 min under vacuum at each temperature stage (25, 40, 60, 80, 100 and 120 °C) before recording the corresponding FTIR spectrum and then normally cooled down to room temperature under vacuum.

2.4. Conductivity and proton transport number measurements

Before the conductivity and transport number measurements, the tested membranes were soaked in a H_2SO_4 (0.1N) solution for 24 h at 25 °C, then rinsed in pure water and wiped up on both sides.

Electrochemical impedance spectroscopy for conductivity measurements was performed in a cell specially designed in our laboratory to be adapted to not self-supported plasma polymers. It is a two-compartments cell with four platinum electrodes, filled with a H_2SO_4 solution (0.1N); more details relative to the working principle of this cell has been given in a previous paper by our group [29]. The impedance spectra were recorded at 25 °C, in the frequency range 0.1 Hz–1 MHz, with a Solartron 1260 Frequency Response Analyzer connected to a Solartron 1287 Electrochemical Interface Potentiostat supplying the dc bias potential and the ac sinusoidal perturbation. For all experiments, the dc bias potential was maintained at 0 V and the ac perturbation at 10 mV. The study of impedance spectra on the high frequency side enables to determine the resistance (R) of plasma-polymerized membranes; then their conductivity (σ) can be calculated [29].

In order to confirm the ability of plasma polymers to conduct protons, measurements of proton transport number were performed in a Hittorf cell (Fig. 3) at 25 °C. The asymmetrical Teflon cell is composed of two compartments filled wilh a H_2SO_4 solution (0.1N), each containing a stirrer and a platinized titanium electrode; the difference of volume between the anodic compartment (200 mL) and the cathodic one (20 mL) enables to generate a sufficiently important variation of proton concentration. The membrane (plasma polymer deposited on a PVDF substrate) separates both compartments; two Viton seals are positioned on both sides of the membrane. The apparent defined area per membrane was 3.14 cm^2.

The method to determine the proton transport number through the membrane is based on the variation of acid concentration in the cathodic compartment of the cell after the transport of a known electrical charge through the system. A current of 70 ± 0.5 mA was applied for 1 h. Only the oxidation of water on the anodic side and the reduction of proton on the cathodic side occur at the electrodes. It was assumed that the cathodic and anodic reactions had current efficiencies of 100%.

The proton transport number through the membrane, t_{H^+}, is defined as the ratio of the current density transported by the proton, j_{H^+}, to the total current density, j

$$t_{H^+} = \frac{j_{H^+}}{j}. \quad (1)$$

Mass balance for protons in the cathodic compartment enables to express the molar flux of protons through the mem-

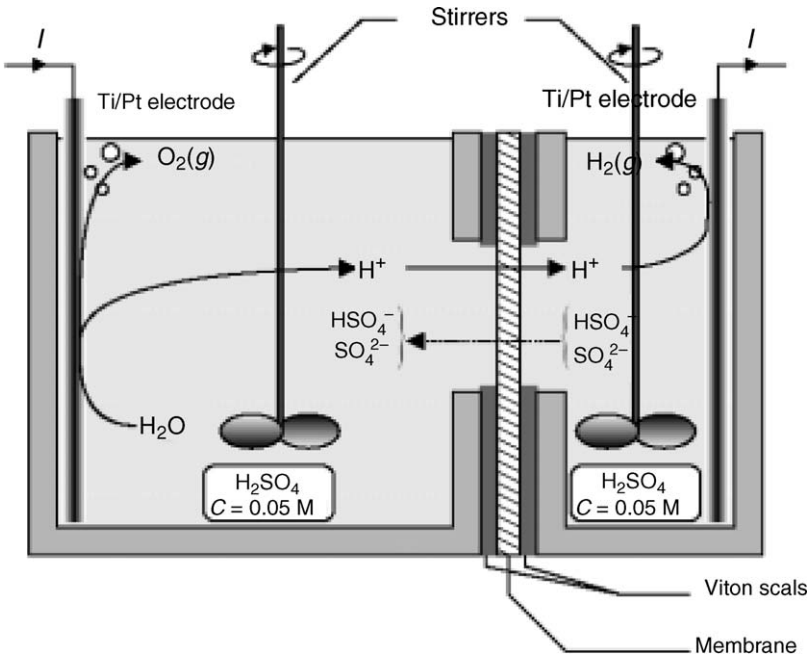

Fig. 3. Hittorf cell for the proton transport number measurements.

brane J_{H^+} by:

$$J_{H^+} = \frac{(\Delta C_{H^+} V)}{\Delta t} + \frac{I}{F} \quad (2)$$

where ΔC_{H^+} is the variation of the molar concentration of protons in the cathodic compartment, V the volume of the cathodic compartment, Δt the experiment duration, I the applied current and F is the Faraday constant. Then, the transport number of proton through the membrane is given by:

$$t_{H^+} = \frac{\Delta C_{H^+} VF}{\Delta t I} + 1. \quad (3)$$

2.5. Methanol sorption measurements

Classical microbalance used for the gas or vapor sorption measurements could not be used for plasma polymers because of their low thickness and mass. The variation of the plasma polymer mass ΔM_S resulting from the dissolution of methanol into the plasma polymers was measured using a very sensitive quartz crystal microbalance MAXTEK TM-400 (sensitivity: 10^{-9} g) depicted in Fig. 4. The plasma polymer was deposited on a quartz substrate coated with Au film (diameter of the sample: 14 mm, thickness: 0.3 mm, frequency: 6 MHz). Sorption measurements were performed with methanol absolute pressure equal to 0.03, 0.07 and 0.1 mbar at 25 °C.

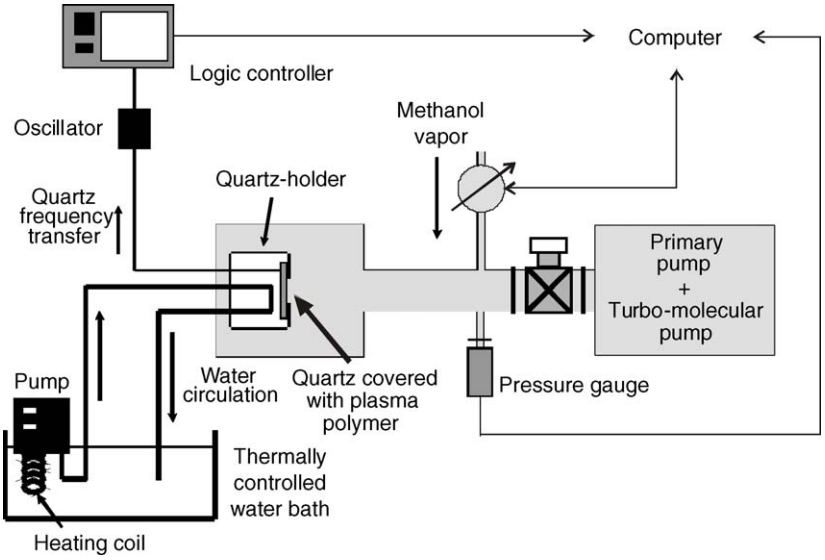

Fig. 4. Experimental set-up for methanol sorption measurements.

The apparatus detects the frequency difference Δf of the piezoelectric crystal which is directly proportional to the variation of the plasma polymer mass ΔM_S obtained from:

$$\Delta M_S = \frac{\rho_q A_q t_q \Delta f}{f} \quad (4)$$

where ρ_q, A_q, t_q and f are the density (g cm^{-3}), the surface (cm^2), the thickness (cm) and the frequency (s^{-1}) of the piezoelectric crystal. The methanol sorption capacity of plasma membranes is quantified by the solubility coefficient S (mol m^{-3} Pa^{-1}), which corresponds to the thermodynamic parameter of the transport and reflects the methanol–membrane interactions:

$$S = \frac{\Delta M_S}{M_{MeOH} P_{MeOH} A d_p} \quad (5)$$

where ΔM_S is the mass of the dissolved gas (g), M_{MeOH} the molar mass of methanol (g mol^{-1}), P_{MeOH} the pressure of methanol (Pa), and A and d_p are the plasma film surface (m^2) and thickness (m), respectively.

2.6. Methanol diffusion permeability measurements

Methanol permeability measurements were realized using a Hittorf type diffusion cell similar to that used for transport number measurements (Fig. 3) but without any electrode in compartments. The membrane (plasma polymer deposited on PVDF substrate) was clamped between donor and receptor compartments with a membrane cross-sectional area of 3.14 cm^2 exposed to the solution. The donor and receptor compartments were initially filled with 200 mL of 5 or 10% methanol aqueous solution and 20 mL of water, respectively. The methanol diffusion coefficients were determined from infrared titration of the solution in the receptor compartment after one hour of dialysis at 25 °C. For this purpose, a calibration curve of the absorbance at 1015 cm^{-1} of the C–O stretching vibration of methanol versus methanol concentration (0.1–2 vol% CH_3OH) was realized.

The flux of methanol J (mol m^{-2} s^{-1}) through the membrane is experimentally evaluated from:

$$J = \frac{x V_R \rho_{MeOH}}{100\ M_{MeOH}\ \Delta t A} \quad (6)$$

where x is the vol% of methanol in the receptor compartment, V_R the volume of the receptor compartment (m^3), ρ_{MeOH} the methanol density (g m^{-3}), M_{MeOH} the molar mass of methanol (g mol^{-1}), Δt the experiment duration (s) and A is the membrane active area (m^2).

The methanol fluxes deduced from the diffusional profile of methanol through the membrane (plasma polymer + PVDF substrate) are given by the following expressions:

$$J = \frac{-D_{PVDF}\ \Delta C_1}{d_{PVDF}} \text{ for the PVDF substrate} \quad (7)$$

and

$$J = \frac{-D_P\ \Delta C_2}{d_P} \text{ for the plasma film} \quad (8)$$

where D_{PVDF} and D_P are the methanol diffusion coefficients of the PVDF substrate and the plasma film, respectively, ΔC_1 and ΔC_2 are the methanol concentration gradients through the PVDF substrate and the plasma film, respectively, d_{PVDF} and d_P are the thickness of the PVDF substrate and the plasma film, respectively.

A first experiment performed with the virgin PVDF substrate without any plasma film enables to calculate D_{PVDF} from the experimental determination of J (Eq. (6)) and the use of Eq. (7). The experimental determination of J (Eq. (6)) with a second experiment performed with the global membrane (plasma film + PVDF substrate), the use of Eqs. (7) and (8) and $\Delta C = \Delta C_1 + \Delta C_2$, leads to the determination of the methanol diffusion coefficient (m^2 s^{-1}) of the plasma film D_P. An intrinsic adimensional coefficient (noted I.C.) was expressed as the ratio of the methanol diffusion coefficient of plasma polymer to the diffusion coefficient of Nafion® N-117 membrane; an absolute adimensional coefficient (noted A.C.) was expressed as the ratio of the methanol flux through plasma polymer to the methanol flux through Nafion® N-117 membrane.

3. Results and discussion

3.1. Characterization of the plasma phase

The mass spectrum of the styrene vapor without any plasma is presented in Fig. 5(a). Unfortunately high fragmentations of the initial monomers occur in the ionization chamber of the mass spectrometer, even if a low electron impact energy is selected (25 eV) in order to minimize this fragmentation and emphasize the fragmentation due to electron impacts in the plasma phase. The main characteristic mass peaks are at $m/z = 104$ amu, corresponding to the parent C_8H_8, at 78 amu (recombined C_6H_6), at 77 amu (phenyl group, $^{\bullet}C_6H_5$) and at other lighter masses corresponding to $[C_MH_N]^{P\bullet}$ radicals typically seen in (un)saturated linear or cyclic hydrocarbons mass spectra. Fig. 5(b) represents the CF_3SO_3H mass spectrum; it also shows that strong fragmentations and recombinations occur in the mass spectrometer. Fig. 6 depicts the mass spectrum of the styrene/CF_3SO_3H gas mixture (1/6 partial pressures ratio). The aspect is close to that of the styrene mass spectrum except for the peaks at $m/z = 57, 69$ and 91 amu, corresponding to radicals formed by the recombination of the initial fragments. This reflects the catalysis effect of the sulfonic acid on the styrene polymerization. In order to study the fragmentation process of the monomers mixture styrene/CF_3SO_3H (1/6 partial pressures ratio) subjected to Ar plasma, the mass spectrometry analysis was performed during the introduction of these monomers in the discharge volume, on the one hand without any plasma in the reactor chamber (plasma "OFF"), on the other hand with a plasma in the reactor chamber (plasma "ON"). The results relative to dissipated powers equal to 7 and 40 W are presented in Fig. 7. For a better visualization of the plasma effect, the difference between the plasma "OFF" and the plasma "ON" spectra has been displayed. Small masses have positive values on the intensity axis, while high masses have negative values, proving that the fragmentation rate of monomers is higher in the presence of plasma.

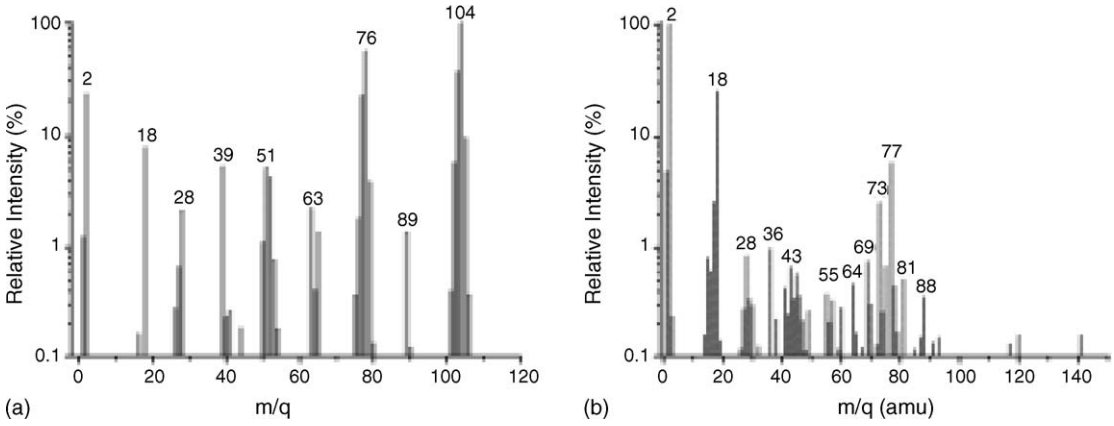

Fig. 5. Mass spectra of styrene (a) and CF_3S0_3H (b).

Only fragments relative to styrene and argon can be observed. It seems that CF_3SO_3H could not be transported to the mass spectrometer's probe in the presence of argon certainly due to the high condensability of CF_3SO_3H when compared to argon. With increasing the dissipated power in the discharge from 7 to 40 W, the fragmentation degree increases, notably leading to the disappearance of phenyl ring-based fragments (78 and 104 amu) coming from styrene at 40 W. This result confirms the choice of a post-discharge configuration (enabling low dissipated powers) for the plasma polymerization of our monomers mixture, whose structure has to be as preserved as possible during the synthesis process.

3.2. Morphology and chemical structure of plasma polymers

3.2.1. Morphology and density

From a previous work, it has been shown that StCF1 and StCF3.5 plasma polymers are uniform, flat, free from defects and strongly adherent on every kind of substrate [29]. Similar characteristics can be observed for StCF4.5 film; the SEM pictures of this film deposited on a silicon wafer and an E-TEK support are shown in Fig. 8. Thus, the morphologic properties of the plasma polymers obtained are independent on the partial pressure of CF_3SO_3H during the deposition process.

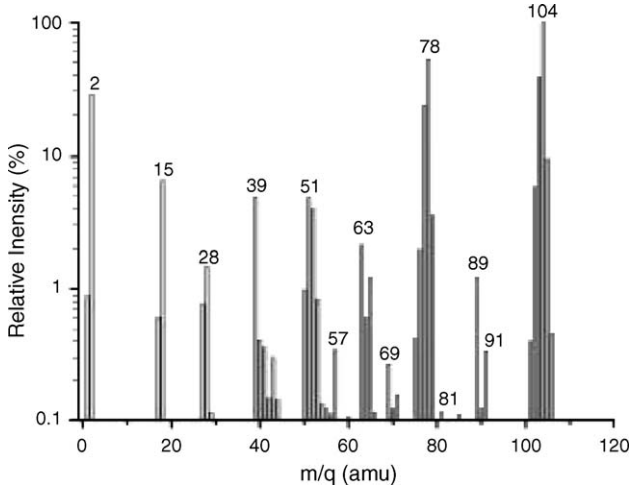

Fig. 6. Mass spectrum of styrene/CF_3SO_3H gas mixture (1/6 partial pressures ratio).

The densities of StCF1, StCF3.5 and StCF4.5 films determined from small-angle X-ray reflectometry measurements are equal to 1.4, 1.3 and 1.3 g cm^{-3}, respectively. Comparatively, the density of conventional polystyrene is 1.05 g cm^{-3}, this of conventional sulfonated polystyrene with Li^+ as counter ion is 1.17 g cm^{-3}. The much higher density values of plasma polymers are directly dependent on the high degree of cross-linking characteristic of this kind of materials. Nevertheless, the measured density values are relatively low by comparison with the majority of plasma-polymerized materials. This data reveals that plasma polymers synthesized from CF_3SO_3H and styrene have a relatively "airy" structure certainly due to the presence of phenyl rings coming from styrene (as has been shown in our previous paper [29]) and playing the role of chains spacers in polymers.

3.2.2. FTIR analysis

Fig. 9 shows the FTIR spectra of StCF1, StCF3.5 and StCF4.5 films recorded at 25 °C. The assignment of the bands relative to StCF1 and StCF3.5 films has already been reported in our previous paper [29]. A very similar assignment can be made for the spectrum of the StCF4.5 film. Spectra of plasma polymers show two different kinds of bands. The first kind of bands is relative to chemical bonds coming from the fragmentation of styrene and constituting the network of the polymer matrix: signature of phenyl rings at 3060, 3080, 1600, 1490, 759 and 699 cm^{-1}, signature of aliphatic carbonated chains at 2960, 2927, 2844, 1450, 1370 and 1030 cm^{-1}. As for he StCF3.5 film [29], a further band at 841 cm^{-1} assignable to CH out-of-plane vibration of para-disubstituted benzene appears in the spectrum of the StCF4.5 film; in the conventional sulfonated polystyrene this absorbance band indicates that sulfonation occurs in the para position of benzene rings [30,31]. The second kind of bands, concentrated in the region 1420–1030 cm^{-1}, is relative to chemical bonds characteristic of sulfonated or fluorinated groups, coming from the fragmentation of trifluoromethane sulfonic acid.

In accordance with mass spectrometry observations, these FTIR data prove the high preservation of the monomers structure in plasma polymers, for monomers subjected to a slightly

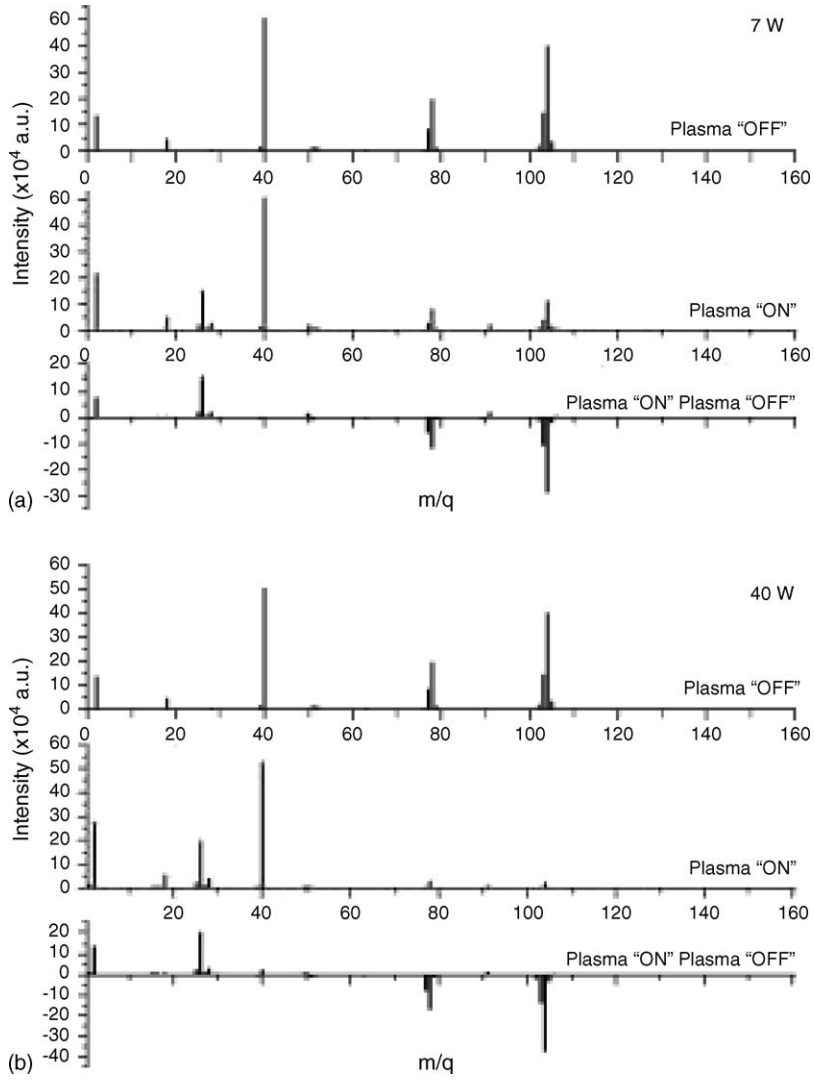

Fig. 7. Effect of an Ar plasma on the fragmentation of a styrene/CF_3SO_3H gas mixture (1/6 partial pressures ratio). Dissipated power equal to (a) 7 W and (b) 40 W.

powerful discharge as it is the case in a post-discharge configuration.

The comparison of bands intensities on FTIR spectra of plasma polymers shows that the StCF3.5 film is the one showing the highest relative intensities for bands relative to sulfonated groups when compared to relative intensities of bands relative to phenyl rings. The XPS analysis should enable to confirm that the StCF3.5 film is precisely the film having the highest proportion of sulfonic acid groups.

Fig. 10 shows the FTIR spectra of the StCF4.5 film at 25 °C, at the maximum temperature of the thermal treatment described in Section 2.3 (120 °C) and lastly at 25 °C after normal cooling under vacuum. One cannot observe major changes in position and intensity of bands relative to aliphatic or aromatic carbon-

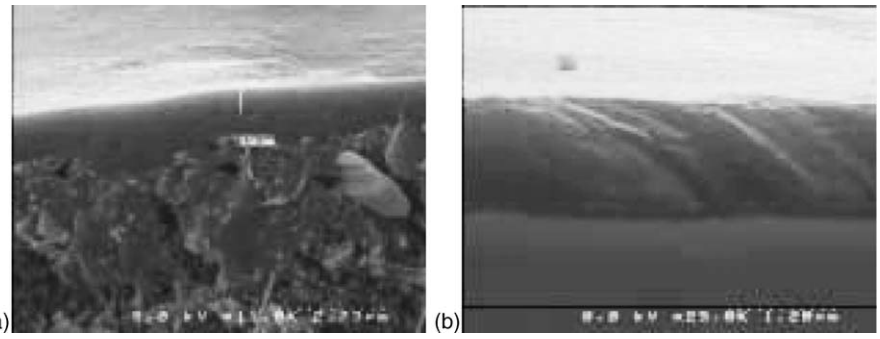

Fig. 8. Scanning electron micrographs of the StCF4.5 film deposited on a E-TEK support (a) and on a silicon wafer (b).

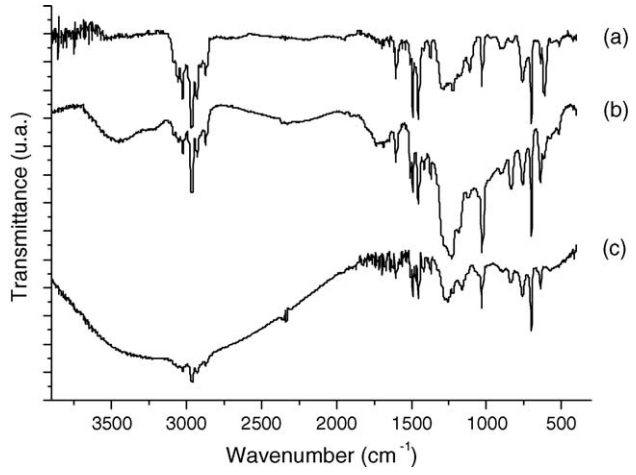

Fig. 9. FTIR spectra of plasma polymers: (a) StCF1 (thickness: 1.1 μm), (b) StCF3.5 (thickness: 1.4 μm) and (c) StCF4.5 (thickness: 1 μm).

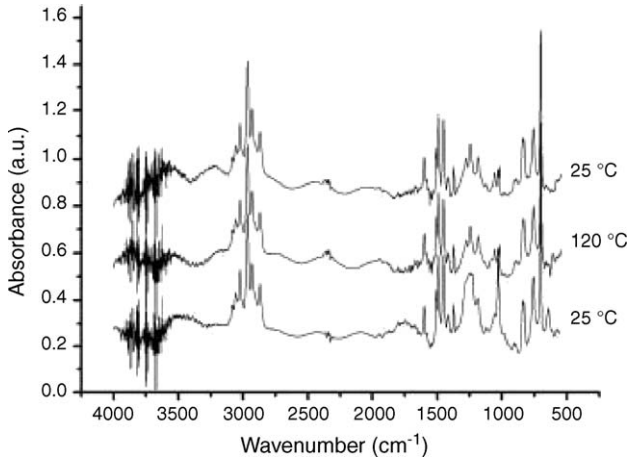

Fig. 10. FTIR spectra of the StCF4.5 film at the beginning (25 °C), top value (120 °C) and end (after cooling down to 25 °C) of the temperature treatment.

ated chains, which proves that no thermal degradation in the plasma polymer structure takes place up to 120 °C. Nevertheless, the broad band in the region 1420–1030 cm^{-1}, notably comprising contributions from $–SO_3^-$ stretching vibrations, has a strong evolution with temperature increasing as can be more precisely observed in Fig. 11. The sulfonate anion SO_3^- is a highly polarizable group, being very sensitive to its environment [32]. The position and intensity of its stretching vibrations can give information on local symmetry of this anion and types of interactions in which this anion is implicated. Two different kinds of local symmetry can be distinguished. The C_{3v} local symmetry (symmetric stretching vibration at 1030 cm^{-1}, asymmetric stretching vibration at 1200 cm^{-1}) is relative to "free" $–SO_3^-$ groups; in this case, the negative charge is uniformly distributed among all S–O bonds and consequently the $–SO_3^-$ has a regulate pyramidal structure. The C_s local symmetry is relative to "associated" $–SO_3^-$ groups, attached to counter-ions ($–SO_3^-$, A^+) or implicated in covalent bonds ($–SO_2OR$). In the case of attachment to a counter-ion, the symmetric stretching vibration of $–SO_3^-$ is represented by an absorption band at 1057 or 1088 cm^{-1} depending on the kind of counter-ion attached, while the asymmetric stretching vibration appears on the form of two absorption bands at 1188 and 1244 cm^{-1}. In the case of implication in $–SO_2OR$ groups, a band relative to asymmetric SO_2 stretching vibration can be found at 1415 cm^{-1}. One can observe in Fig. 11 that at room temperature, there are six absorption bands relative to $–SO_3^-$ stretching vibrations, corresponding to "free" $–SO_3^-$ groups (1030 and 1200 cm^{-1}), $–SO_3^-$, A^+ groups (1057, 1188 and 1244 cm^{-1}) and $–SO_2OR$ groups (1415 cm^{-1}). With temperature increasing: the band at 1030 cm^{-1} decreases, the band at 1200 cm^{-1} splits, bands at 1188 and 1244 cm^{-1} increase and a new band arises at 1088 cm^{-1}. Theses evolutions can be explained by the following simultaneous phenomena: change of "free" $–SO_3^-$ groups in $–SO_3^-$, A^+ groups, change of $–SO_3^-$, A^+ groups in "free" $–SO_3^-$ groups or change of the type of A^+ (with stronger electrostatic field than those present at 25 °C) in $–SO_3^-$, A^+ groups. After cooling down to 25 °C, the band at 1088 cm^{-1} disappears, which proves the semi-reversibility of the temperature effect. All these observations suggest that the temperature effect on the plasma polymers structure corresponds to some ionic rearrangements of sulfonate anions with the aim of always finding the minimal energy of interaction with the polymer matrix environment and/or the associated counter-ions.

3.2.3. XPS analysis

S_{2p}, spectra of StCF1, StCF3.5, StCF4.5 plasma polymers and Nafion® N-117 were studied to investigate the chemical state of sulfur in materials structure. As has been shown in our previous paper [29], the S_{2p} spectra of plasma polymers can

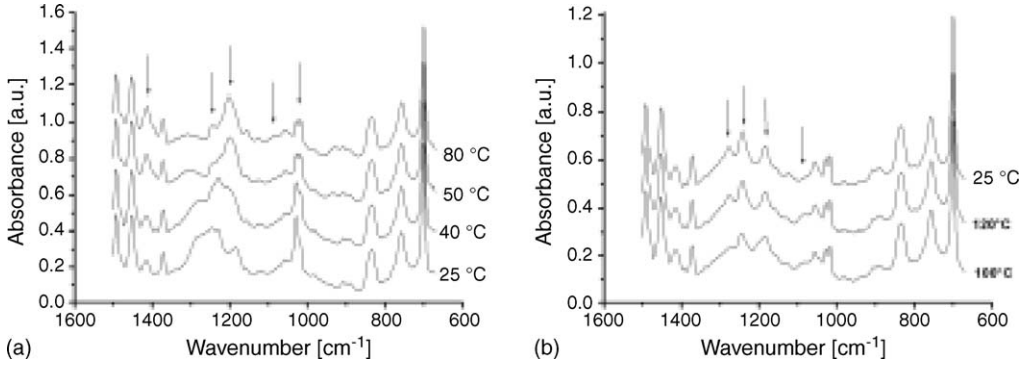

Fig. 11. FTIR spectra of the StCF45 film in the range 600–1500 cm^{-1} as a function of temperature.

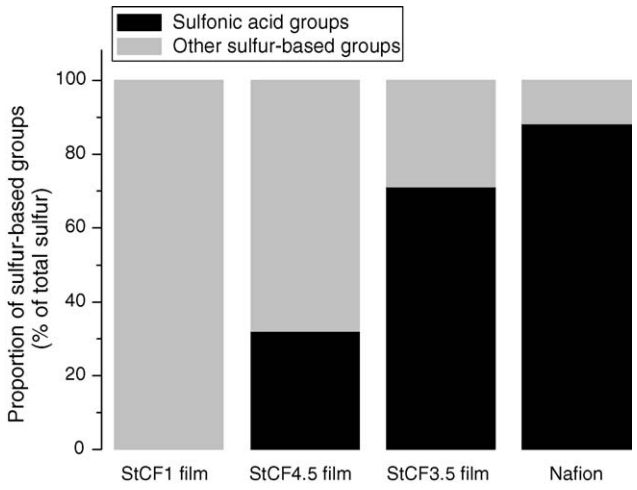

Fig. 12. XPS proportion of sulfur-based groups in StCF1, StCF3.5 and StCF4.5 films (percentage of total sulfur). Comparison with Nafion® N-117.

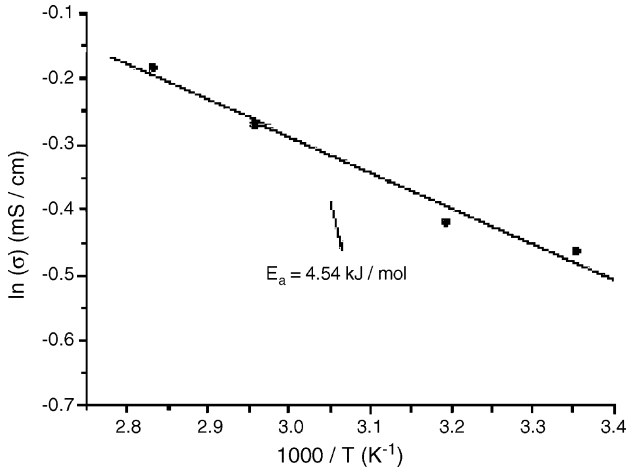

Fig. 13. Arrhenius plot of proton conductivity of the StCF3.5 film as a function of temperature.

be deconvolved into four components: 170 and 169 eV both assigned to sulfonic acid groups, 166 and 164.5 eV assigned to groups of lower oxidation states (essentially sulfone groups). Fig. 12 shows the percentage of total sulfur incorporated as sulfonic acid and other sulfur-based groups in StCF1, StCF3.5 and StCF4.5 films, deduced from the peak area values; comparison is made with Nafion® membrane. With identical partial pressures of CF_3SO_3H and styrene in the monomers mixture (StCF1 film), 100% of the total sulfur is present as sulfur-based groups different from sulfonic acid ones. In contrast, the StCF3.5 film contains the highest proportion of sulfonic acid groups (71% of total sulfur). For the StCF4.5 film, synthesized from the monomers mixture characterized by the highest CF_3SO_3H concentration, only 32% of total sulfur is present as sulfonic acid groups. Consequently, the atomic percentage of sulfonic acid groups related to the total atom quantity is 0% pour the StCF1 film and the highest one, 5.0%, for the StCF3.5 film. When the quantity of CF_3SO_3H introduced in the reactor is maximum (StCF4.5 film), the sulfonic acid content is only 2.3%. The comparison between the three films reveals that increasing the proportion of CF_3SO_3H in the monomers mixture do not systematically increase the sulfonic acid content in plasma polymers. The comparison with Nafion® N-117 (sulfonic acid groups content: 1.1%) makes suppose that good proton conductivities for StCF3.5 and StCF4.5 films can be expected, more particularly for the first one.

3.3. Proton transport properties of plasma polymers

The transport numbers of proton through StCF3.5 and StCF4.5 plasma polymers, equal to 0.836 and 0.841 respectively, are similar and relatively high. This result is the proof that both plasma polymers are good proton conductors. The StCF3.5 film, which contains the highest sulfonic acid content, logically shows the highest intrinsic conductivity: 9.8×10^{-2} mS cm^{-1} [29]. The low proton conduction capacity of plasma-polymerized membranes when compared to Nafion® N-117 (9.6 mS cm^{-1} in the same experimental cell) is mainly due to their low swelling directly related to their high cross-linking degree. Although not very conductive, these membranes exhibit specific resistances similar (2 Ω cm^2 for 2 μm thick films) and even lower (1 Ω cm^2 for 1 μm thick films) than Nafion® (1.9 Ω cm^2) because of their adjustable low thickness. Fig. 13 presents the temperature dependence of the conductivity for the StCF3.5 plasma-polymerized membrane (temperature range between 25 and 80 °C). The natural logarithms of measured conductivity values as a function of temperature values were fitted with an Arrhenius-type equation:

$$\sigma = \sigma_0 \exp\left(\frac{-E_a}{RT}\right) \tag{9}$$

where σ is the proton conductivity (mS cm^{-1}), σ_0 the preexponential factor (mS cm^{-1}), E_a the activation energy for proton conduction (J mol^{-1}), R the pure gas constant and T is the temperature (K). According to the Hopping model [33], the preexponential factor σ_0 depends on the carrier concentration, the activation entropy ΔS and the hopping frequency ν_0 between sites separated by the distance d:

$$\sigma_0 = \left(\frac{z^2F^2\alpha\nu_0 d^2}{R}\right) \exp\left(\frac{\Delta S}{R}\right) \tag{10}$$

where z is the number of electrons changed in reaction, F the Faraday constant, R the pure gas constant and α is the reciprocal of the number of every likely hopping direction.

It seems interesting to investigate the proton conduction mechanism in plasma polymers. Generally, two different kinds of proton conduction mechanism are distinguished in polymer membranes: the Grotthus mechanism (that assumes that the proton jumps from the lone pair of electrons of a water molecule to the lone pair of electrons of a neighboring water molecule, with successive formations and deformations of H_3O^+ ions) and the vehicle mechanism (that assumes that the proton combines with a water molecule to form H_3O^+ which is transported by diffusion through the material). Well hydrated polymers are expected

Table 1
Methanol permeability properties of plasma polymers (comparison with Nafion® N-117)

	Thickness (μm)	Density (g cm^{-3})	Initial concentration in the donor compartment (vol% MeOH)	Methanol diffusion coefficient (m^2 s^{-1})	I.C.	Methanol flux (mol m^{-2} s^{-1})	A.C.
Nafion®	185	–	5	1.37×10^{-10}	1	0.91×10^{-3}	1
			10	1.36×10^{-10}	1	1.81×10^{-3}	1
StCF1	0.24	1.4	5	1.85×10^{-13}	1.35×10^{-3}	0.95×10^{-3}	1.04
			10	2.21×10^{-13}	1.63×10^{-3}	2.28×10^{-3}	1.26
StCF3.5	0.22	1.3	5	2.06×10^{-13}	1.50×10^{-3}	1.15×10^{-3}	1.26
			10	2.30×10^{-13}	1.69×10^{-3}	2.58×10^{-3}	1.43
StCF4.5	0.38	1.3	5	3.65×10^{-13}	2.66×10^{-3}	1.18×10^{-3}	1.30
			10	4.51×10^{-13}	3.32×10^{-3}	2.93×10^{-3}	1.62

to conduct by the Grotthus mechanism because the Grotthus mechanism requires close proximity of water molecules which are firmly held but able to rotate; polymers with less amount of water would be expected to conduct by the vehicle mechanism [34]. In Nafion® is suggested that both mechanisms co-exist, with a predominance of the Grotthus mechanism characterized by an activation energy around 10–40 kJ mol^{-1} [35–40]. Also in plasma polymers, the Grotthus mechanism can be considered as predominant; indeed the highly cross-linked structure of plasma polymers is certainly very unfavorable to the vehicle mechanism. The activation energy (E_a) for proton conduction of the StCF3.5 plasma-polymerized membrane, calculated from the linear least-square fits to the experimental temperature dependence of conductivity (Fig. 13), is equal to 4.54 kJ mol^{-1}. The fact that the energy barrier for proton conduction is lower for plasma polymers than for Nafion® could be explained by an easier structural reorganization under the effect of temperature, due to the existence of more electrostatic driving forces, as has been evidenced by FTIR analysis.

3.4. Methanol transport properties of plasma polymers

3.4.1. Methanol sorption

In order to determine the solubility mechanism in plasma polymers, measurements were realized at different methanol pressures. It was observed a linear relationship between the concentrations of gas dissolved in the plasma polymer and the gas pressure inside the chamber; this indicates a pseudo-Henry law which is currently the case for gas or polar vapor.

The solubility coefficients S measured at a methanol pressure of 0.1 bar are 0.1, 0.21 and 0.14 mol m^{-3} Pa^{-1} for StCF1, StCF3.5 and StCF4.5 membranes, respectively. We can observe that the solubility coefficients of the plasma polymers are directly linked to the sulfonic acid contents determined by XPS analysis (0%, 5.0% and 2.3% for StCF1, StCF3.5 and StCF4.5 films, respectively). This results from the affinity of methanol with the polar groups –SO_3^- present in the plasma-polymerized films. Thus, the film showing the lowest methanol solubility is the film showing the lowest sulfonic acid content (StCF1 film). The same kind of dependence between the sulfonic acid content and the methanol solubility coefficient was observed at methanol pressures of 0.03 and 0.07 bar.

3.4.2. Methanol diffusion permeability

In Table 1 are reported the diffusion coefficients (intrinsic property of material), the methanol fluxes (extrinsic property of material) and the I.C. and A.C. coefficients of plasma polymers and Nafion® N-117. The thickness and density of materials are also listed in this table. The methanol fluxes and diffusion coefficients are slightly different depending on the initial concentration of methanol in the donor compartment for a same material. This is related to the underestimation of such parameters (all the more pronounced as the initial concentration is low) due to the decrease of the methanol concentration in the donor compartment as the diffusion test is going on. Results in Table 1 show that plasma polymers are intrinsically much less permeable to methanol than the Nafion® membrane; the I.C. coefficients are between 1.35×10^{-3} and 3.32×10^{-3}. This can be explained by the highly cross-linked structure of plasma polymers. From an absolute point of view, the tested plasma polymers which are particularly thin due to the specific nature of the PVDF support show methanol fluxes slightly higher than that of Nafion®; the A.C. coefficients are between 1.04 and 1.62. Nevertheless, by increasing the deposition duration, it is possible to deposit thicker plasma films showing lower methanol fluxes than that of Nafion®. The use of 2 μm thick plasma-polymerized membranes could induce a reduction of the methanol crossover in factors 7–11.

The plasma-polymerized film showing the lowest methanol permeability (the lowest retention coefficient) is the film with the highest density (StCF1 film). It is well known that the higher is a material cross-linked; the lower is the gas or vapor mobility in this material.

From the methanol transport results, it can be concluded that the StCF1 film shows the best barrier effect to methanol because of its higher density (1.4) and its sulfonic acid content equal to zero. For the same reasons, it's also the film characterized by the lowest conductivity.

4. Conclusion

Proton-exchange sulfonated polystyrene-type membranes were synthesized by plasma polymerization of a styrene/trifluoromethane sulfonic acid monomers mixture in a low-frequency after-glow discharge process. Mass spectrometry

analysis enabled to show that low discharge power values are required to preserve the monomers structure and consequently to incorporate a lot of phenyl rings and sulfonic acid groups in plasma polymers, likely to favor the ionic conduction. Such low discharge power values are easy to obtain with an after-glow discharge process, such as that used in this study. The synthesized plasma-polymerized membranes are dense and uniform with a few microns thickness. Their structure determined by FTIR and XPS analyses is stable up to 120 °C; it is made up of a carbonated matrix composed of phenyl groups and containing a proportion of proton-exchanger sulfonic acid groups (up to 5%) higher than Nafion® N-117 in optimized synthesis conditions. In spite of high sulfonic acid groups content, plasma-polymerized membranes are intrinsically less conductive (10^{-1} S cm^{-1}) than Nafion® N-117 due to their disorganized and highly cross-linked structure. Although not very conductive, these membranes yet exhibit specific resistances (around 2 Ω cm^2 for 2 μm thick films) similar to Nafion® N-117 (1.9 Ω cm^2) because of their low thickness. Due to their highly cross-linked structure, these membranes show permeability to methanol around 1000 times lower than that of Nafion® N-117; the use of 2 μm thick plasma membranes can induce a reduction of the methanol crossover in a factor 10 by comparison with Nafion® N-117.

Thus, sulfonated polystyrene-type plasma-polymerized membranes present very interesting properties for an application in miniaturized fuel cells (especially DMFCs): high compacity, high chemical and thermal stability, satisfying protonic conduction level and very low permeability to methanol. Moreover, their manufacture cost is rather low. From now on, it is possible to envisage the integration of such membranes in an "all solid" 100 μm thick compact heart of cell which would comprise all the active layers (electrodes, catalytic layer, membranes) synthesized by dry deposition techniques. This study is going on with this aim of integration.

Acknowledgments

The authors are very grateful to Didier Cot and Arie van der Lee from the Institut Européen des Membranes, Montpellier (France), and René Berjoan from the Institut des Matériaux et Procédés, Odeillo (France), for performing SEM observations, small-angle X-ray reflectometry analyses, and XPS measurements, respectively. The authors also thank the GDR "PACEM" no. 2479 (French research program) for its financial support.

References

[1] L.J. Hobson, H. Ozu, M. Yamaguchi, S. Hayase, J. Electrochem. Soc. 148 (10) (2001) A1185–A1190.
[2] W.C. Choi, J.D. Kim, S.I. Woo, J. Power Sources 96 (2001) 411–414.
[3] S.R. Yoon, G.H. Hwang, W.I. Cho, I.-H. Oh, S.-A. Hong, H.Y. Ha, J. Power Sources 106 (2002) 215–223.
[4] M. Walker, K.M. Baumgärtner, Surf. Coat. Technol. 116–119 (1999) 996–1000.
[5] M. Walker, K.M. Baumgärtner, M. Kaiser, J. Kerres, A. Ullrich, E. Raüchle, J. Appl. Polym. Sci. 74 (1999) 67–73.
[6] Z. Ogumi, Y. Uchimoto, M. Tsujikawa, Z.I. Takehara, F.R. Foulkes, J. Electrochem. Soc. 137 (5) (1990) 1430–1435.
[7] Z. Ogumi, Y. Uchimoto, M. Tsujikawa, Z.I. Takehara, J. Electrochem. Soc. 136 (1989) 1247–1248.
[8] R. Zeng, Z. Pang, H. Zhu, J. Electroanal. Chem. 490 (2000) 102–106.
[9] K. Yasuda, T. Yoshida, Y. Uchimoto, Z. Ogumi, Chem. Lett. 10 (1992) 2013–2016.
[10] P. Dimitrova, K.A. Friedrich, U. Stimming, B. Vogt, Solid State Ionics 150 (2002) 115–122.
[11] B. Baradie, J.P. Dodelet, D. Guay, J. Electroanal. Chem. 489 (2000) 101–105.
[12] V. Mehta, J.S. Cooper, J. Power Sources 114 (2003) 32–53.
[13] Y.A. Elabd, E. Napadensky, J.M. Sloan, D.M. Crawford, C.W. Walker, J. Membr. Sci. 217 (2003) 227–242.
[14] N. Carrerta, V. Tricoli, F. Picchioni, J. Membr. Sci. 166 (2000) 189–197.
[15] M.V. Fedkin, X. Zhou, M.A. Hofmann, E. Chalkova, J.A. Weston, H.R. Allcock, S.N. Lvov, Mater. Lett. 52 (2002) 192–196.
[16] H.Y. Chang, C.W. Lin, J. Membr. Sci. 218 (2003) 295–306.
[17] B. Bae, D. Kim, J. Membr. Sci. 220 (2003) 75–87.
[18] L.J. Hobson, Y. Nakano, H. Ozu, S. Hayase, J. Power Sources 104 (2002) 79–84.
[19] J. Kerres, W. Zhang, A. Ullrich, C.-M. Tang, M. Hein, V. Gogel, T. Frey, L. Jörissen, Desalination 147 (2002) 173–178.
[20] V. Tricoli, N. Caretta, Electrochem. Commun. 4 (2002) 272–276.
[21] J. Kim, B. Kim, B. Jung, J. Membr. Sci. 207 (2002) 129–137.
[22] K. Yasuda, Y. Uchimoto, Z. Ogumi, Z.-I. Takehara, J. Electrochem. Soc. 141 (1994) 2350–2355.
[23] Y. Uchimoto, K. Yasuda, Z. Ogumi, Z.-I. Takehara, J. Electrochem. Soc. 138 (1991) 3190–3193.
[24] C.J. Brumlik, A. Parthasarathy, W.-J. Chen, C.R. Martin, J. Electrochem. Soc. 141 (1994) 2273–2278.
[25] N. Inagaki, S. Tasaka, T. Kurita, Polym. Bull. 22 (1) (1989) 15–20.
[26] M. Walker, K.-M. Baumgärtner, J. Feichtinger, M. Kaiser, E. Raüchle, J. Kerres, Surf. Coat. Technol. 116–119 (1996) 996–1000.
[27] J. Feichtinger, R. Galm, M. Walker, K.-M. Baumgärtner, A. Schulz, E. Raüchle, U. Schumacher, Surf. Coat. Technol. 142–144 (2001) 181–186.
[28] F. Finsterwalder, G. Hambitzer, J. Membr. Sci. 185 (2001) 105–124.
[29] H. Mahdjoub, S. Roualdès, P. Sistat, N. Pradeilles, J. Durand, G. Pourcelly, Fuel Cells 5 (2) (2005) 277–286.
[30] J.J. Fitzgerald, R.A. Weiss, ACS Symp. Ser. 302 (1986) 35–53.
[31] H.-M. Liu, J.-C. Liu, F.-M. Zhu, S.-A. Lin, Polym. Int. 50 (4) (2001) 421–428.
[32] G. Zundel, Hydration and Intermolecular Interactions, Academic Press Inc., New York, 1969.
[33] G. Alberti, U. Constantino, M. Casciola, S. Ferroni, L. Massinelli, P. Staiti, Solid State Ionics 145 (2001) 249–255.
[34] A. Clearfield, Chem. Rev. 88 (1988) 125–148.
[35] B. Smitha, S. Sridhar, A.A. Khan, Macromolecules 37 (2004) 2233–2239.
[36] K.D. Kreuer, Chem. Mater. 8 (2004) 610–641.
[37] M. Doyle, M.E. Lewittes, M.G. Roelofs, S.A. Perusich, J. Phys. Chem. B 105 (2001) 9387–9394.
[38] X. Zhou, J. Weston, E. Chalkova, M.A. Hofmann, CM. Ambler, H.R. Allcock, S.N. Lvov, Electrochim. Acta 48 (2003) 2173–2180.
[39] Y.A. Elabd, E. Napadensky, J.M. Sloan, D.M. Crawford, C.W. Walker, J. Membr. Sci. 217 (2003) 227–242.
[40] N. Carretta, V. Tricoli, F. Picchioni, J. Membr. Sci. 166 (2000) 189–197.